Impact resistance and recovery in SMA stitched E-glass reinforced Poly(ε-caprolactone)/epoxy composites

Amaël Cohades[1], Malvina Pauchard[1] and Véronique Michaud[1]

[1] Laboratory for Processing of Advanced Composites (LPAC), Institute of Materials, Ecole Polytechnique Fédérale de Lausanne (EPFL), CH-1015 Lausanne, Switzerland,
veronique.michaud@epfl.ch, http://lpac.epfl.ch

Keywords: Self-healing composites, Shape-memory alloys, Thermoplastic/thermoset blends, Impact testing, Crack closure

ABSTRACT

Damage recovery after low-velocity impact has been assessed in Shape Memory Alloy (SMA) wires stitched woven E-glass fibre-reinforced polymer composites. The matrix was epoxy (two types: a low and high toughness one) or a blend of epoxy and 25vol% of poly(ε-caprolactone) (PCL). SMA stitched wires (sewn across the dry fibres) were introduced to potentially close cracks through their shape memory effect whereas epoxy-PCL blends were used to heal low damage volumes formed within the remaining crack space, thanks to the PCL expansion and melting capacity at moderate temperatures. Composites were processed by vacuum assisted resin infusion moulding to reach a fibre volume fraction around 50%. Impact was carried out at three energy levels (8.5, 17 and 34 Joules) and even though the damage extent was higher in composites with the epoxy-PCL matrix, these demonstrated similar energy absorption capacity as compared to pure epoxy composites. The extent of damage (determined by optical images) was quantified for the different impact energy levels, before and after thermal mending at 150°C for 30 minutes in order to assess the material's capacity to reduce the damage area. While SMA stitched composites with the low toughness epoxy matrix showed a damage area recovery from 56 up to 63% depending on the impact energy level, SMA stitched composites with the high toughness resin did not show damage reduction after thermal treatment. The efficiency of transverse SMA wires to close cracks in composites could therefore not be concluded from this optical analysis due to a low optical contrast during crack closure. Extending this concept to the epoxy-PCL matrix showed damage reduction (up to full recovery for impacts at 8.5 Joules energy); the efficiency of this healing process will be further evaluated and quantified using ultrasonic scanning techniques.

1 INTRODUCTION

Glass fibre reinforced polymer (FRP) composite structures may be subjected during service to low energy impacts or unexpected loads, leading to damage. For example, low-velocity impacts in aircrafts are damage events due to operational or maintenance activities and are of main concern because these tend to decrease strength, durability and stability of the structure [1]. Several methods (see for example [2]) are currently in practice or under development to repair damage events in composite structures, but these are often complicated and time consuming, especially when the damage is barely visible. Microcracks are generally first formed in the matrix and can reach up several hundred microns in thickness. In order to efficiently heal these cracks before further propagation, an ideal system would (i) be based on a healing matrix that can also expand and fill submicron cracks; and (ii) autonomously close cracks that are above a threshold thickness, to ensure contact between the faces to heal.

Considerable effort has been made over the last 25 years to integrate a self-healing functionality into thermoset polymers for the autonomous repair of sub-critical damage. Two categories of systems have been developed: (i) extrinsic systems, which consist of capsules or vascules integrated into the thermoset matrix and which will rupture during crack propagation and release a healing agent that will

flow and polymerize into the damage volume [3]; (ii) intrinsic systems, which use an alternative matrix that has the intrinsic ability to heal [4]. Both approaches have demonstrated their interest into neat resin [3], but remain more challenging and less investigated so far when integrated to FRPs. In extrinsic systems, where healing capsules are used, the integration to FRPs has been well demonstrated, however due to a too large damage volume to be filled by the capsule content, these systems showed a loss in mechanical properties (both when assessing interlaminar crack opening [5,6] and impact induced damage [7]). Extrinsic systems where vascules are integrated to FRPs have the ability to deliver large quantities of resin into the damage volume, and have demonstrated full restoration of damage events after impacts up to 20 Joules; however, these systems are not able to provide multiple healing to a single damage as well as to provide healing of low damage levels that do not cross a vascule. For the intrinsic approach, a strategy to restore damage even where crack faces are not in contact consists in preparing an immiscible blend [8,9] between a thermoset and a low melting point semicrystalline thermoplastic. In that case, healing involves different mechanisms: (i) melting and consequent volume expansion of the thermoplastic; (ii) flow of the thermoplastic melt into the damage zone; (iii) physical or chemical healing at the molecular level. This type of healing is repeatable as it implies the recovery of thermodynamic equilibrium in the thermoplastic phase; however, it requires damage to propagate through the thermoplastic phase or along the interface between the thermoplastic and the thermoset. Two of the studied systems have demonstrated their potential for use in FRPs: (i) the systems studied by Pingkarawat *et al.* [10] (FRPs with a matrix consisting of a blend of epoxy and the ionomeric copolymer polyethylene-co-methacrylic acid (EMAA)) where recovery up to 156% has been demonstrated in Mode I double cantilever beam (DCB) testing, and (ii) the systems studied by Cohades *et al.* [11,12] (FRPs with a matrix consisting of a blend of epoxy and poly(ε-caprolactone) (PCL)) where full recovery of damage events after impacts up to 8.5 Joules has been demonstrated. Both systems are based on a differential expansive bleeding mechanism where the thermoplastic has the ability to expand and bridge the crack faces. Nonetheless, both systems are able to bridge cracks thickness up to some tenths of microns only.

In order to increase the efficiency of the mentioned systems, a strategy would be to add a functionality that would autonomously close cracks that are above a threshold thickness and which would ensure closer contact between the faces to heal. For example, shape memory alloy (SMA) wires inserted inside FRPs through stitching of the dry fabric before processing could bring crack faces closer. After damage and upon heating SMA stitches, that have been stretched and partly debonded upon crack propagation, these could recover their initial length and/or exert a stress reaching several hundred MPa, thus allowing to efficiently close the cracks before the healing matrix system would take place. This strategy has been modelled by Bor et al. [13] to show promise to close delamination at interfaces. SMA wires, inserted in between plies of FRPs, have shown increased energy absorption capability [14,15], however, no insertion as stitches to close cracks can be found in the available literature.

In the present study, we investigated a combined healing strategy applied to FRP with two functionalities: (i) epoxy-PCL blends as matrix to provide healing and (ii) stitched NiTiCu SMA wires to close cracks. Blends of epoxy and 25 vol% of PCL in neat resins have demonstrated over 70% recovery in Mode I testing [8] as well as toughness, stiffness and compression strength recovery in FRPs up to respectively 45%, 100% and 100% [11,12] after a thermal mending cycle at 150°C for 30 minutes while retaining suitable strength, stiffness and toughness properties at room temperature. In this system, the healing ability is provided through a phase separation mechanism which creates a microstructure consisting of interconnected epoxy particles (keeping the load bearing capacity) and a surrounding PCL matrix (which has the ability to expand by 14% upon melting at 150°C, thus bridging the crack faces). Adding SMA wires as stitches in FRPs in combination with an epoxy-PCL(25vol%) healing matrix is therefore believed to enhance crack healing through the combined action of the PCL expansion and SMAs crack closure. We present here low-velocity impact tests at three different impact energy levels and the assessment of damage area recovery of these smart systems after a thermal mending cycle at 150°C for 30 minutes by means of optical microscopy. To understand the effect of SMAs on the damage area reduction, three matrices have been used: (i) a low

toughness epoxy (i.e. 0.85 MPa $m^{1/2}$) (ii) a high toughness epoxy (i.e. 1.45 MPa $m^{1/2}$) and (iii) the healing epoxy-PCL matrix (epoxy being the high toughness one).

2 MATERIALS AND METHODS

2.1 Materials

Epon™ 828EL (Momentive), a widely available diglycidyl ether bisphenol A (DGEBA) resin with a molar mass of 340.41 g/mol and a molar mass per epoxide group of 185-192 g/eq was cured either with 4,4'-diaminodiphenylsulfone (DDS 98 %, *ABCR*, molar mass = 248.3 g/mol, 2:1 molar ratio with respect to the epoxy) or with diethylenetriamine (DETA, *Sigma Aldrich*, 100:12 weight ratio with respect to the epoxy). The epoxy cured with DDS was also blended with PCL (*Capa™ 6500*, $M_w \approx$ 50,000 g/mol, *Perstorp*). Three types of resin have thus been prepared: (i) pure epoxy resin cured with DETA (this resin is the low toughness resin), (ii) pure epoxy resin cured with DDS (this resin is the high toughness resin) and (iii) epoxy-PCL blends containing 25vol% of PCL and cured with DDS. The PCL volumetric ratio was determined for the liquid blends, assuming a density of 1.145 g/cm^3 for the PCL and a density of 1.34 g/cm^3 for the epoxy-DDS. The glass fibre reinforcement was a woven twill 2x2 E-glass fabric, with a nominal areal weight of 390 g/m^2, 6 end/cm for warp fibres and 6.7 picks/cm for weft fibres, fibre diameter of 9 µm, yarn thickness of 0.45 mm, warp tex of 68x5 and weft tex of 272, from *Suter-Kunststoffe AG*. The SMA wire used was a martensitic NiTiCu alloy with relative composition 44.86/45.08/10.06 and a diameter of 150µm (*Furukawa Techno Material*).

2.2 Samples preparation and processing

The composite plates were processed by Vacuum Assisted Resin Infusion Moulding (VARIM). Sixteen layers of fibre reinforcement were cut in 350x250 mm rectangles and stacked with a sequence of $[(+45/-45)/(0/90)_2/(+45/-45)]_4$, similar to our previous study [12]. This stack was further stitched with SMA wires using a commercial *Singer* (model 632G) sewing machine and using a jean needle. Lines spaced each 4 mm were drawn on the fabric to ease alignment during the stitching process (Fig. 1 (a)) and a target distance between two stitched knots of 4 mm has been set through the speed and wire tension on the machine. This stitching pattern corresponds to 700 SMAs/m^2 which can theoretically provide recovery forces up to 4000 N/m^2. The reproducibility achieved through such a semi-automatic process is depicted on Fig. 1 (b) and the mean achieved values between two stitched lines and two knots were respectively of 4.49 ± 0.75 mm and 3.94 ± 0.78 mm. A target fibre volume fraction (V_f) of 50 vol% and a final plate thickness of 5 mm were sought. The preforms to be infused were prepared following the lay-out as depicted in Fig. 2. But before any bagging, the stitched preforms were placed at 150°C for 30 minutes in order to (i) remove internal stresses from the sewing process and (ii) have the SMA wires in a fully detwinned martensitic state which provides theoretically the maximum shape memory effect. In order to ease resin infusion, the inlet has been placed at the middle of the infusion design and the flow medium both at the top and bottom of the reinforcement.

Infusion with the low toughness resin (i.e. epoxy-DETA) has been performed at room temperature and was then cured at room temperature for 24h followed by a post-cure at 45°C for 24h. Infusion with the high toughness resin (i.e. epoxy-DDS) and blends of epoxy with 25vol% PCL were prepared following a procedure described in our previous studies [8,12]. The liquid epoxy and the PCL pellets were first melt-mixed in glass jars at 120 °C by mechanical stirring at 100 rpm for 1 h with a three-blade propeller (*Caframo*, Canada, 1", 5/16" bore). After 1 hour, the temperature was increased to 140 °C, the stirring rate was increased to 400 rpm, and DDS (in powder form) was slowly added to the mixture. When the mixture became transparent, it was degassed at 120 °C for 20 min and infused into the composite in an oven set to 140°C, which ensured a blend viscosity below 1 Pa·s [12]. The composite then underwent a curing treatment at 180°C for 3h, which previously showed full resin polymerization [8,12]. Samples from the three systems were cut from the produced plates (dimensions are given in Fig. 2) using a Maïco saw equipped with a diamond blade. For each sample, the weight was recorded, the thickness measured in 3 points, averaged and the fibre volume fraction calculated. In

addition, for every epoxy-PCL composite process, a small droplet of the blend has been placed in between two glass slides in order to control by optical microscopy (Olympus BX-60) that the same morphology as in our previous studies [8,12] (i.e. epoxy particles with a surrounding PCL matrix) was obtained.

SMA stitched composites made of (i) pure epoxy (low toughness one, epoxy-DETA) are named "*DETA"* in the following and contained a fibre volume fraction of 48.19 ± 0.41% and a SMA volume fraction of 0.40 ± 0.001%; (ii) pure epoxy (high toughness one, epoxy-DDS) are named "*DDS"* in the following and contained a fibre volume fraction of 46.68 ± 0.71% and a SMA volume fraction of 0.33 ± 0.02% and (iii) epoxy-PCL blends are named "*PCL(25)*" in the following and contained a fibre volume fraction of 47.03 ± 1.07% and a SMA volume fraction of 0.41 ± 0.01%.

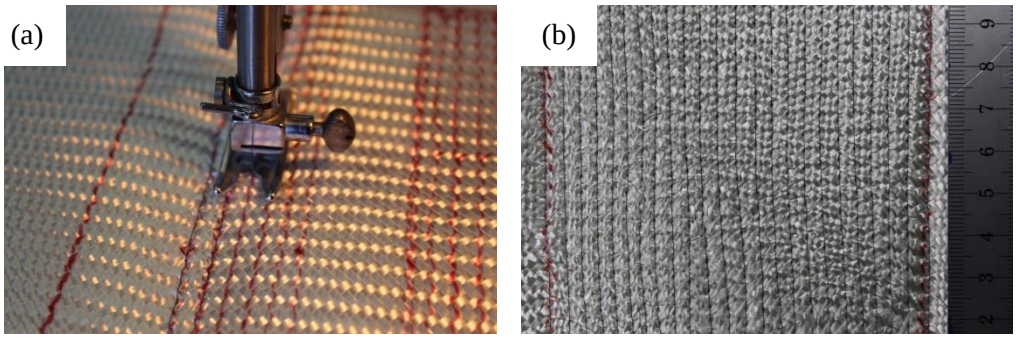

Figure 1: Illustration of **(a)** the stitching process on the stacked preform and **(b)** the dry preform after stitching.

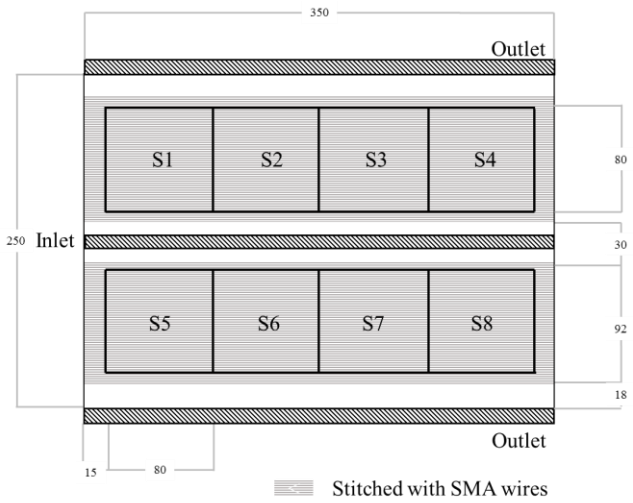

Figure 2: Schematic top view of the VARIM lay-out, including the fibre preform unstitched with SMA wires (white), the fibre preform stitched with SMA wires (grey lines pattern) the inlet and outlet lines. Note that a flow mesh has been place at the top and bottom of the lay-up to ease infusion. The geometry of impact samples is also showed. Dimensions are in mm.

2.3 Impact testing

The low-velocity impact behaviour of the produced samples was assessed following ASTM 7136 [16] with a *Rosand* impact testing machine. The load imparted by the 5.5 kg impactor was recorded by a 60 kN *Kistler* load cell. Thus, the velocity, impactor displacement as well as energy absorbed as a function of time could be calculated. Also, the velocities before and after impact were measured through light gates placed just above the samples and the energy dissipated within these samples

deduced. The potential energy, *E*, imparted to the specimen prior to drop was measured following the ASTM standard [16]:

$$E = C_E h \quad (1)$$

with C_E the specified ratio of impact energy to specimen thickness, 6.7 J/mm, and h the nominal thickness of the specimen. In order to observe different damage areas, three energies have been tested, corresponding to E, E/2 and E/4 which represent respectively around 34, 17 and 8.5 Joules energies and around 3.0, 2.2 and 1.5 m/s inbound velocities. Notice that because healing is the main concern of this study, the energy was each time adapted to each specimen thickness in order to create the same damage amount. At least 3 samples were tested for each energy and system.

2.4 Damage recovery through optical analysis

Pictures of the samples before and after impact as well as before and after the thermal mending cycle (30 minutes at 150°C) were taken with a *Canon D600* camera and then binarized with *Matlab* software. Pictures before impacts were used as baseline to isolate the impact. The ratio between the area of damage before and after thermal mending was defined as the efficiency in impact damage recovery.

3 RESULTS AND DISCUSSION

3.1 Preliminary study

Preliminary impact experiments have been performed on SMA stitched composites made of a low toughness epoxy resin (epoxy-DETA) which was cured at room temperature and post-cured at 45°C. Impacts have been performed at three different energies (34, 17 and 8.5 Joules) and samples have then been subjected to a heat treatment at 150°C in order to assess the recovery in the damage area quantified by binarized optical images. Binarized images before (*Virgin)* and after (*Heat treated*) the heat treatment are shown for the three impact energies on Fig. 3. The black region is the impacted area, whereas the black lines show the SMA wires stitched within the system. The heat treatment allowed reducing the impacted area by 56.0%, 58.9% and 62.5% for respectively 34 J, 17 J, and 8.5 J. Even though the recovery of the impacted area was not complete, the reduction achieved when inserting SMA wires at 17 J gave a similar impacted area as unstitched samples impacted at 8.5 J. Considering the ability of epoxy-PCL composites to fully recover impacts of 8.5 J energy [11], using SMA wires were expected to improve the healing ability of samples combining a healing matrix and SMA stitches. However, this behavior needed to be confirmed for impact samples containing epoxy-PCL samples (i.e. *PCL(25)* samples) as well as the pure epoxy cured with DDS (i.e. *DDS* samples).

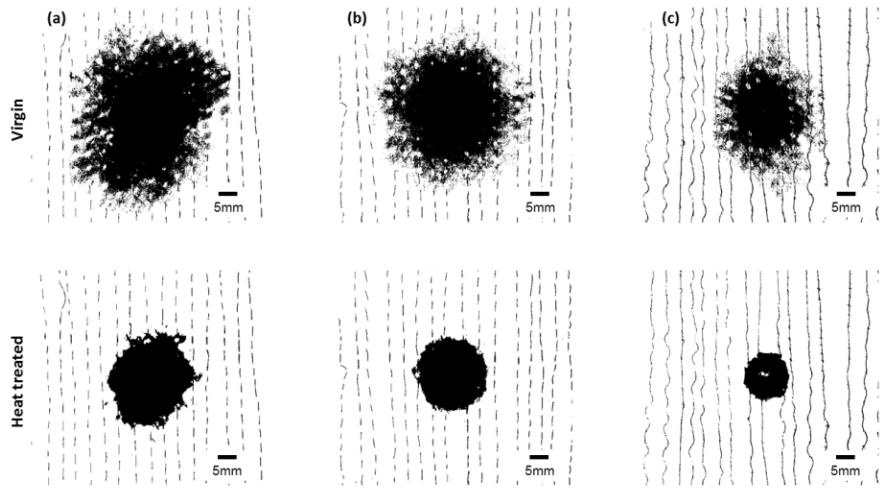

Figure 3: Binarized optical image of impacted *DETA* samples, at impact energies of (a) 34 J, (b) 17 J and (c) 8.5 J. Images are shown before (*virgin*) and after (*heat treated*) a thermal mending cycle of 30 minutes at 150°C.

3.2 Impact testing

The impact forces as well as energy levels during an impact are represented as a function of time for representative samples of *DDS* and *PCL(25)* systems in Fig. 4 (left axis for impact forces and right axis for energy levels). As expected, when the impact energy increased, the peak load as well as the energy during test increased. In both cases, a maximum on the curve can be observed, representative of the maximum penetration depth of the impactor. The load curve shows oscillations before this maximum for both systems (*DDS* and *PCL(25)*) as well as for the three impact energies, while a smooth decrease down to zero load is observed after this maximum. This behaviour is well known in conventional FRPs [1,17]: oscillations are attributed to growing ply delamination during penetration of the impactor within the sample while no further delamination occurs during rebound of the impactor (i.e. after the peak load). Still focusing on the load response, the first oscillation is representative of the first delamination within the sample (also called Hertzian failure [17]) and appeared earlier for *PCL(25)* samples. This behaviour was attributed to the lower resistance to crack propagation (i.e. toughness) as well as to the lower strength of this healing matrix, as determined in our previous studies [8,12]. Another characteristic behaviour of a difference in delamination resistance between these two systems can be highlighted through the time at which the peak load was reached. Indeed, the peak load was reached later in *PCL(25)* samples as compared to the *DDS* samples, which indicated that the healing matrix accumulated more damage due to its lower delamination resistance before rebound of the impactor.

Impact energy levels during tests also increased up to a maximum value, before decreasing and reaching a final value. This decrease corresponds to the energy restituted to the impactor by the sample and the final observed value could be defined as the dissipated energy by the impactor within the impacted sample. The energy levels have been calculated following the ASTM standard D7136 [16], however, this calculation does not consider other energy consumption mechanisms such as friction within the machine guides, energy transferred during test directly to the impactor and the base machine, or deformation of the grips [18]. In order to counter those effects, the inbound and rebound velocities have also been determined in the present study. These are given in Table 1 (as well as mean values of maximum load observed) and the similarity between *DDS* and *PCL(25)* samples was attributed to the fact that energy absorption mechanisms are mainly related to the capacity of the reinforcement fibres to absorb energy [19]. As compared to previously determined data on samples without SMA stitches [11], the dissipated energy increased up to 16% for both assessed systems in the present study. This behaviour was attributed to the presence of SMAs which have well-known damping properties [14,15].

In Table 1, the maximum load and the energy dissipated during impact are given for the three impact energies as well as for the two assessed systems. A relatively high standard deviation can be observed for every value, greater than that achieved with the tests performed previously on the same systems but without SMA stitches [11]. This deviation was attributed to the position of the impact as referred to the position of the SMA stitched lines in the samples. Two extreme cases are shown on Fig. 4 for the *DDS* system: (i) an impact lying exactly on a SMA stitched line (Fig. 4 (a)) and (ii) an impact lying exactly in between two SMA stitched lines (Fig. 4 (b)). The shape of the damage area is different for these two cases: (i) the impact is long and the damage area seems to have followed the stitched line, thus energy dissipation was directed through the SMA stitches, and (ii) the impact has a rounder shape and the damage area seems to have propagated more within the composite. However, the measure of damage areas (through binarization of the optical image, see section 3.3) in every samples for the three impact energies revealed values in the same range whether the impact was lying on a SMA or not. From the present findings, it can be concluded that the impact position with respect to the SMA stitched lines influences the damage shape, and to a lower extent the damage level. This influence may lead to the standard deviation observed within the impact data. Finally, the quality of the stitching pattern achieved with the sewing machine can be observed from Fig. 5.

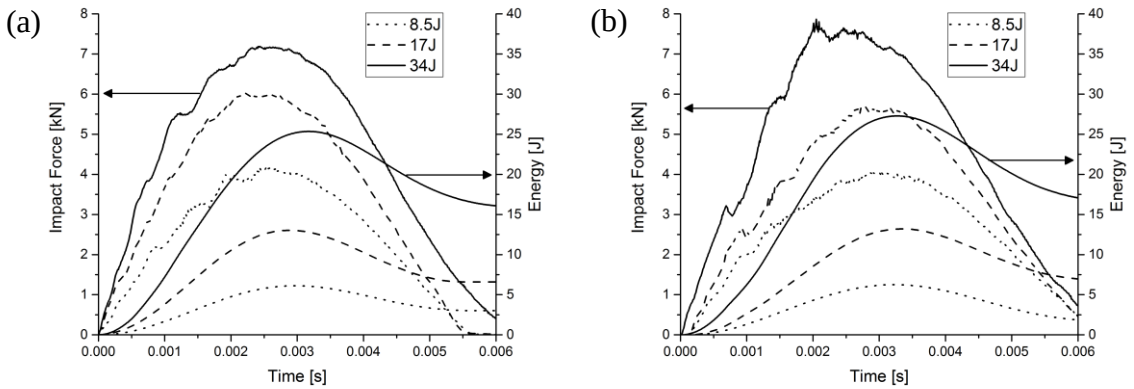

Figure 4: Impact force and energy as a function of time for three different impact energies, for (a) *DDS* samples and (b) *PCL(25)* samples.

Sample	Impact energy [J]	F_{max} [kN]	E_{diss} [J]
DDS	34	7.09 (0.19)	15.96 (0.69)
	17	5.69 (0.28)	6.92 (0.21)
	8.5	4.58 (0.43)	2.46 (0.22)
PCL	34	7.51 (0.27)	16.81 (1.27)
	17	5.67 (0.11)	6.93 (0.63)
	8.5	4.12 (0.55)	3.40 (0.28)

Table 1: Maximum load (F_{max}) and dissipated energy (E_{diss}) during impact at three different energies (34, 17 and 8.5 Joules) for the *DDS* and *PCL* systems.

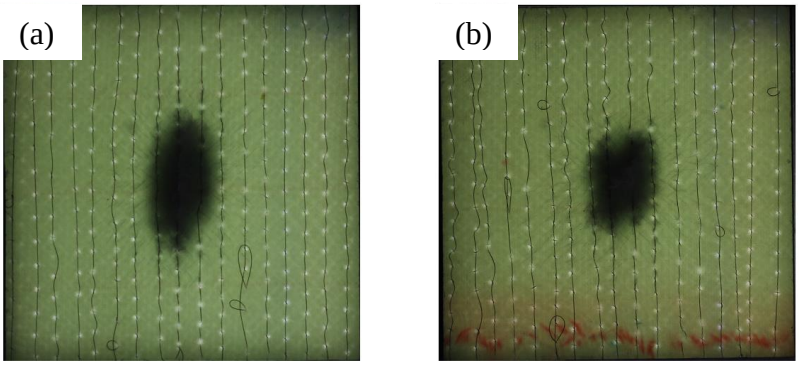

Figure 5: Back face optical image of *DDS* samples impacted at 34 Joules energy: **(a)** impact on a SMA stitched line and **(b)** impact in between two SMA stitched lines.

3.3 Damage recovery through optical analysis

Recovery of impact damage area has been first quantified for *DDS* samples, which were expected to demonstrate the ability of the SMAs to close cracks only. Optical images were binarized and the impact damage isolated; the comparison of the impact area before (*Virgin*) and after (*Heat treated*) thermal mending cycle allowed determination of the SMA capacity to close cracks, which changed the image light contrast and thus the binarization threshold (Fig. 6). This experiment is similar to the preliminary study presented in section 3.1, however the composite was here made of the epoxy matrix used to create the PCL healing blends (i.e. cured with DDS). As this epoxy is tougher than that cured with DETA, the observed damage area on Fig. 6 is smaller as compared to Fig. 3.

Subjecting the samples to a thermal treatment at 150°C for 30 minutes demonstrated little recovery for impacts at 8.5 J whereas no impact damage recovery was observed at high energies. This

behaviour, not in accordance with the preliminary study presented in section 3.1 was attributed to the difference in toughness between the two epoxy matrices, but also to the different curing conditions. Indeed, *DETA* samples have been post-cured at 45°C before impact. Subjecting those samples to a thermal treatment at 150°C after impact could therefore have annealed internal stresses which reduced the damage area. Finally, the contrast obtained by this optical analysis might not have been strong enough to detect visual differences in crack closure within impacted samples.

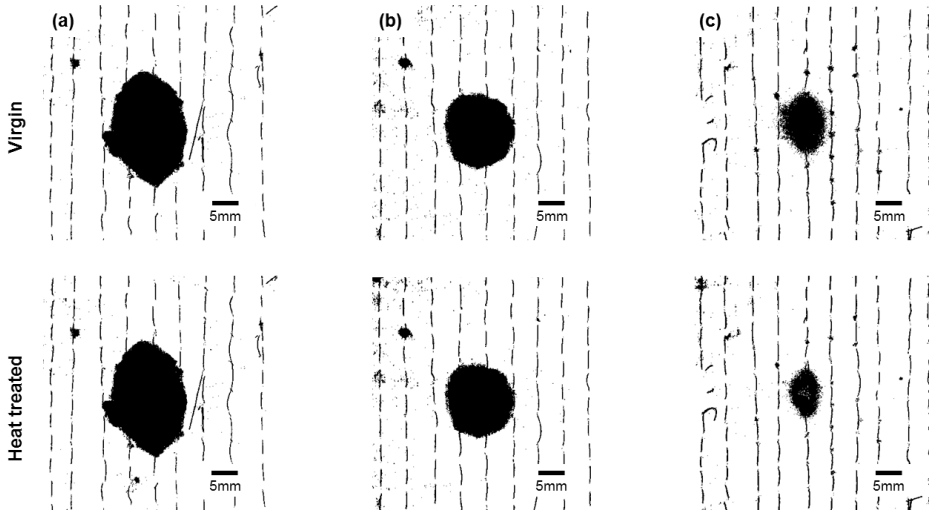

Figure 6: Binarized optical image of impacted *DDS* specimens, at impact energies of (a) 34 J, (b) 17 J and (c) 8.5 J. Images are shown before (*virgin*) and after (*heat treated*) a thermal mending cycle of 30 minutes at 150°C.

Recovery of impact damage area by optical observations was further assessed for *PCL(25)* samples and is shown in Fig. 7 for the three impact energies before (*Virgin*) and after (*Heat treated*) a thermal mending cycle at 150°C for 30 minutes. As compared to *DDS* samples which are relatively transparent to light (see Fig. 5), *PCL(25)* samples are opaque due to the PCL. Full recovery of impact damage was observed for low impact energy (8.5 Joules) whereas at higher impact energy, a trace of the impact, even though smaller than the initial impact, was still present after the thermal mending cycle. Incomplete recovery at high impact energy levels was attributed to fibre rupture and larger crack formation which could not be healed due to the limited expansion capacity of PCL. Isolating the impact damage through binarization was not possible for *PCL(25)* due to the opacity of the samples and thus no healing efficiency could be quantified. No conclusion can therefore be drawn on the SMA crack closure ability as compared to the PCL healing capacity as: (i) the crack closure behaviour in pure epoxy composites (with *DETA* and *DDS* samples) could not be confirmed and (ii) the impact could not be isolated, thus no healing efficiency quantified. Quantifying the ability of SMA stitches to close cracks in composites through optical image observation is thus limited by the contrast difference in transparent as well as in opaque samples, a technique like C-scan would thus be of higher interest to exactly determine the damage contour.

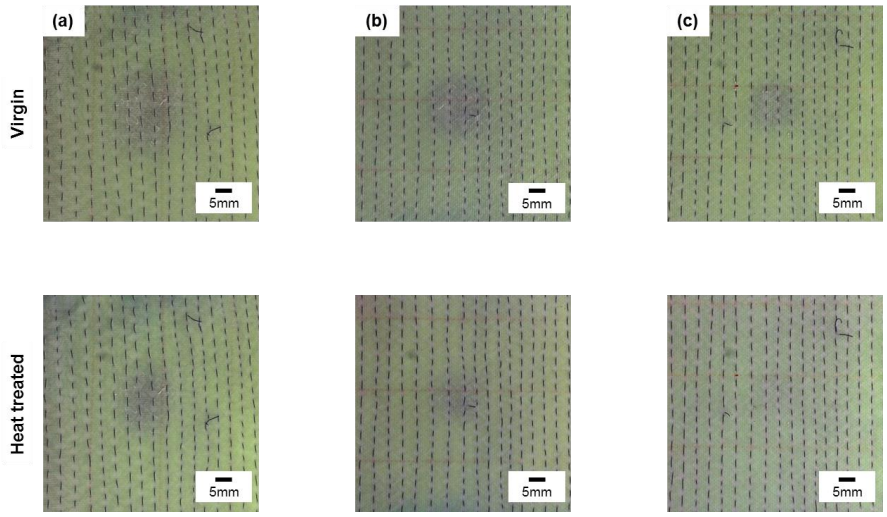

Figure 7: Front face optical image of impacted *PCL(25)* specimens, at impact energies of (a) 34 J, (b) 17 J and (c) 8.5 J. Images are shown before (*virgin*) and after (*heat treated*) a thermal mending cycle of 30 minutes at 150°C.

4 CONCLUSION

SMA stitched glass fibre reinforced epoxy-PCL composites with fibre volume fractions around 50vol% were successfully processed through sewing of the SMA wires on the dry fabric and then through vacuum assisted resin infusion moulding at elevated temperature. Samples were used to characterize their impact response as well as their potential for damage area recovery. As compared to samples with a pure epoxy matrix, samples with the healing matrix (epoxy-PCL(25vol%) blend) demonstrated a lower resistance to crack propagation because Hertzian failure appeared earlier and damage accumulation was higher. This behaviour, expected from our previous studies [8,11,12], was attributed to the lower intrinsic strength and toughness of the healing matrix. Furthermore, the position of the impact with respect to the SMA stitched lines was observed to influence the damage shape, but to a lower extent the damage level. The energy absorption ability was also increased as compared to samples without stitched SMA wires, demonstrating the damping properties of these alloys.

The importance of the matrix resistance to crack propagation was further confirmed by optical image analysis of the impacts where composites with a low toughness epoxy matrix (*DETA*) demonstrated larger damage areas as compared to samples with a higher toughness epoxy matrix (*DDS*). Whereas the impact damage area was reduced for composites with the low toughness matrix, it was not the case for the higher toughness matrix which was attributed to the different curing conditions and the poor light contrast difference obtained in the optical images. Full recovery of impact damage was observed in *PCL(25)* samples for low impact energy (8.5 Joules) whereas at higher impact energy, a trace of the impact (even though smaller than the initial impact) was still present after the thermal mending cycle. Incomplete recovery at high impact energy levels was attributed to fibre rupture and larger crack formation which could not be healed due to the limited expansion capacity of PCL. No difference could be drawn between the SMA crack closure ability and the PCL healing capacity due to the poor light contrast preventing the determination of an exact damage contour. Quantifying the ability of SMA stitches to close cracks in composites through optical image observation is thus limited by the contrast difference in transparent as well as in opaque samples; a technique like C-scan will be used to determine exactly the damage contour. This procedure will allow understanding the capacity of the SMA stitches to close cracks in FRPs and prove their interest in composite structures that are subjected to moderate loads and not easily accessible to repair.

ACKOWLEDGMENTS

This work is funded by the Swiss National Science Foundation (SNF 200020-150007-1). We would like to thank Perstorp for providing the PCL.

REFERENCES

[1] Schoeppner GA, Abrate S. Delamination threshold loads for low velocity impact on composite laminates. Compos Part A Appl Sci Manuf 2000;31:903–15.
[2] Myhre SH, Labor JD. Repair of advanced composite structures. J Aircr 1981;18:546–52.
[3] Blaiszik BJ, Kramer SLB, Olugebefola SC, Moore JS, Sottos NR, White SR. Self-Healing Polymers and Composites. Annu Rev Mater Res 2010;40:179–211.
[4] Garcia SJ. Effect of polymer architecture on the intrinsic self-healing character of polymers. Eur Polym J 2014;53:118–25.
[5] Kessler M., White S. Self-activated healing of delamination damage in woven composites. Compos Part A Appl Sci Manuf 2001;32:683–99.
[6] Manfredi E, Cohades A, Richard I, Michaud V. Assessment of solvent capsule-based self-healing for woven E-glass fibre-reinforced polymers. Smart Mater Struct 2015;24:1–11.
[7] Patel AJ, Sottos NR, Wetzel ED, White SR. Autonomic healing of low-velocity impact damage in fiber-reinforced composites. Compos Part A Appl Sci Manuf 2010;41:360–8.
[8] Cohades A, Manfredi E, Plummer J-C, Michaud V. Thermal mending in immiscible poly(ε-caprolactone)/epoxy blends. Eur Polym J 2016;81:114–28.
[9] Meure S, Varley RJ, Wu DY, Mayo S, Nairn K, Furman S. Confirmation of the healing mechanism in a mendable EMAA-epoxy resin. Eur Polym J 2012;48:524–31.
[10] Pingkarawat K, Bhat T, Craze D a., Wang CH, Varley RJ, Mouritz a. P. Healing of carbon fibre–epoxy composites using thermoplastic additives. Polym Chem 2013;4:5007.
[11] Cohades A, Michaud V. Damage recovery after impact in E-glass reinforced Poly(ε-caprolactone)/epoxy blends SUBMITTED. Compos Struct 2016.
[12] Cohades A, Michaud V. Thermal mending in E-glass reinforced Poly(ε-caprolactone)/epoxy blends, In Press, Accepted Manuscript. Compos Part A Appl Sci Manuf 2017;99:129–38.
[13] Bor TC, Warnet L, Akkerman R, de Boer a. Modeling of Stress Development During Thermal Damage Healing in Fiber-reinforced Composite Materials Containing Embedded Shape Memory Alloy Wires. J Compos Mater 2010;44:2547–72.
[14] Pappadà S, Gren P, Tatar K, Gustafson T, Rametta R, Rossini E, et al. Mechanical and Vibration Characteristics of Laminated Composite Plates Embedding Shape Memory Alloy Superelastic Wires. J Mater Eng Perform 2009;18:531–7.
[15] Michaud V. Can shape memory alloy composites be smart? Scr Mater 2004;50:249–53.
[16] ASTMD7136. Standard Test Method for Measuring the Damage Resistance of a Fiber-Reinforced Polymer Matrix Composite to a Drop-Weight Impact Event. ASTM Stand 2015:1–16.
[17] Shyr T-W, Pan Y-H. Impact resistance and damage characteristics of composite laminates. Compos Struct 2003;62:193–203.
[18] Uyaner M, Kara M. Dynamic Response of Laminated Composites Subjected to Low-velocity Impact. J Compos Mater 2007;41:2877–96.
[19] Cantwell WJ, Morton J. The impact resistance of composite materials - a review. Composites 1991;22:347–62.